International Journal of Turbulence Explorations

SCIEPublish

Article

Reconstructing Fluid Dynamics with Micro–Finite Elements

Wennan Zou *

Institute of Fluid Mechanics, Nanchang University, Nanchang 330031, China

* Corresponding author. E-mail: zouwn@ncu.edu.cn (W.Z.)

Received: 16 July 2026; Revised: 10 August 2026; Accepted: 28 August 2026; Available online: 21 September 2026

ABSTRACT: In the theory of Navier–Stokes (N–S) equations, an incompressible fluid in motion is modeled as a homogeneous and dense assemblage of constituent "fluid particles" with viscous stress proportional to the rate of strain. The crucial concept in fluid flow is the velocity of a particle, which is accelerated by the pressure and viscous interactions around it. In this paper, by virtue of an alternative constituent "micro-finite element", we introduce a set of new intrinsic quantities, called the vortex fields, to characterize the relative orientation between elements and the feature of micro-eddies in the element, while the description of viscous interaction in the fluid returns to that the interlayer friction is proportional to the slip strength, more matching Newton's original intuition. Such a framework enables us to reconstruct the dynamics theory of viscous fluid, in which the fluid can be modeled as a finite covering of elements and consequently its flow is indicated by a space-time differential manifold that admits complex topological evolution.

Keywords: Fluid dynamics; Micro–finite element; Vortex fields; Slip viscosity; Space–time differential manifold

1. Introduction

The fundamental hypothesis underlying fluid dynamics is that the matter of which the fluid is made up is continuously distributed and that the field variables involved, such as velocity, pressure, mass density, *etc*., are continuous functions of space and time. Some people believe that such a macroscopic theory of fluid flow is unique, as what the Navier–Stokes (N–S) equations stand for [1,2]. Previously, the theory of elasticity with the so–called micro–finite elements [3] was recasted, where the elements have the property of intrinsic stretch and may be finitely chosen to cover the elastic body, implying the non-uniqueness of macroscopic models of elastic deformation, and the equivalence of two kinds of theories of elasticity when some reasonable compatibility conditions have been applied. But when a theory of fluid dynamics is elaborated with micro–finite elements (Figure 1) in a similar way, the fluid element has to be defined in a local space-time domain of fluid while such a material element always keeps to be a micro–ellipsoid during the finite elastic deformation process of solid [4], and finally the fluid in motion, as a finite covering of fluid elements if both the space and time are finite, is represented as a four dimensional space-time manifold. As can be demonstrated in the main text, except for the straight laminar flows, say Couette/Poiseuille flows between parallel planes, Poiseuille flow in a straight tube of circular cross-section, *etc*., we find that (i) the possibility is no longer exists to degenerate the new theory to the classical one; (ii) the viscous interaction

© 2026 The authors. This is an open access article under the Creative Commons Attribution 4.0 International License (https://creativecommons.org/licenses/by/4.0/).

in fluid could be reckoned as an internal friction instead of an analogy of elastic stress [5]. Thus, we obtain a completely different macroscopic flow theory for micro-finite fluid elements with viscous friction proportional to slip strength, whilst the N–S equations represent only a flow theory for infinitesimal fluid particles with viscous stress proportional to the rate of strain.

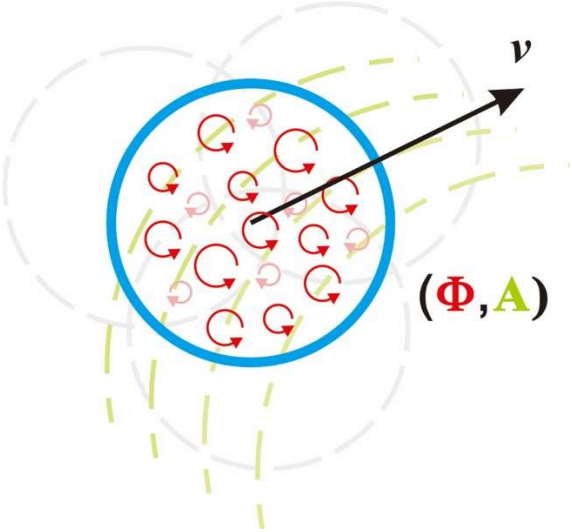


Figure 1. Sketch of the micro-finite element.

In this paper, all quantities and equations are established under the Galilean space–time $E_4 = \mathbb{R}^3 \times \mathbb{R} = \{x_1, x_2, x_3, x_4 = t | x_\mu \in \mathbb{R}, \mu = 1, 2, 3, 4\}$ where (x_1, x_2, x_3) is a Cartesian coordinate system and t stands for the time. The bases $\{\mathbf{e}_1, \mathbf{e}_2, \mathbf{e}_3\}$ of tangent space $T(E_3)$ are referred to as $\mathbf{e}_\mathrm{i} = \partial \mathbf{r}/\partial x_i$ from the position vector $\mathbf{r}$. The natural bases for the vector space $\Lambda^1(E_4)$ of all 1-forms are given by $\{dx_1, dx_2, dx_3, dx_4 = dt\}$. A vector/form is denoted by a minuscule Latin bold letter or by its components, for instance $\mathbf{r}$ or x_i. Summation over repeated indices is tacit, from 1 to 3 for Roman indices and 1 to 4 for Greek indices. The generated bases, called the area elements and volume element, for the vector spaces $\Lambda^2(E_3)$ and $\Lambda^3(E_3)$ of spatial forms are spanned by

$$da_i = \frac{1}{2}\varepsilon_{ijk} dx_j \wedge dx_k, dv = dx_1 \wedge dx_2 \wedge dx_3, \tag{1}$$

respectively, where ε_{ijk} is the permutation symbol of three–dimensional spaces, and '$\wedge$' stands for the exterior product. The superscript index is used for the axial vector, such as angular velocity, moment of force, *etc*.

In the classical fluid dynamics, it is confirmed that the transformation of an addition of constant velocity onto the fluid does change the acceleration and the viscous stress determined by the velocity gradient, and so has no effect on the dynamical process of the situation. But as Figures 6.2 and 6.3 of [6] shown, the contact relation or slip state in the fluid described by the streamlines becomes quite different for the two flows after an inertial transformation. According to the new theory, the viscous interaction between the interlayers of the fluid, if measurable, will recognize a unique investigator seeing the truthful flow velocity, which is called the *macroscopic velocity* v_i. In the following derivation, it is more profitable to introduce the micro-displacement $\mathbf{u}_i = v_i dt$ as a quantity.

2. Flow Fields and Their Intensities

When the fluid under consideration is incompressible and viscous, as water or air flowing in everyday life, the element defined everywhere has no difference from the view of elasticity. Quite different from the elastic deformation, no micro–finite element with internal shear in the flow can be traced and identified

globally. The fluid in motion is then the result of pasting together micro–finite elements defined in local space–time [7]. The velocity v_i, now confined to be the uniquely–determined macroscopic velocity, is just the extrinsic property of flowing elements. Besides, once the shear–induced order [8,9] has been formed and/or the micro–eddies are wheeling, the vortex fields are naturally introduced to characterize the relative orientation between neighboring elements and the micro–rotation in the element, which are regarded as the structural and intrinsic properties of elements in flow.

The vortex fields are indicated by an axial-vector valued differential 1–form

$$\mathbf{W}^i = W_4^i dx_4 + W_k^i dx_k = \Phi^i dt + \mathbf{A}^i, \mathbf{A}^i = A_k^i dx_k, \tag{2}$$

where the temporal part Φ^i is referred to as the micro–eddy field, while the spatial part A_k^i the swirl field. Mathematically, the vortex fields are used to define the connection on the frame bundle of the fluid manifold, which is

$$D\mathbf{e}_i = \varepsilon_{ijk}\mathbf{W}^j\mathbf{e}_k, \tag{3}$$

where D is the covariant exterior differential operator. Using the swirl field, one can calculate the slip strength by

$$D(\mathbf{u}_i\mathbf{e}_i) = (Dv_i)\mathbf{e}_i \wedge dt = Y_{ki}\mathbf{e}_i dx_k \wedge dt, \tag{4}$$

where

$$Y_{ki} = D_k v_i = \partial_k v_i + \varepsilon_{ilm}A_k^l v_m \tag{5}$$

is also referred to as the velocity intensity. For the Newtonian fluids, the viscous friction can be formulated as

$$\boldsymbol{\sigma} = \mu * D(\mathbf{u}_i\mathbf{e}_i) = \mu(D_k v_i)\mathbf{e}_i da_i = \mu\big(\partial_k v_i + \varepsilon_{ilm}A_k^l v_m\big)\mathbf{e}_i da_i, \tag{6}$$

where the operator '$*$' for any base form b is defined by

$$b \wedge * \, b = dv \wedge dt. \tag{7}$$

The topological structures of the connection are essentially determined by the curvature tensor, namely, the vortex intensity defined by

$$\mathbf{F}^i = D\mathbf{W}^i = d\mathbf{W}^i + \varepsilon_{ijk}\mathbf{W}^j \wedge \mathbf{W}^k = B_k^i da_k + H_k^i dx_k \wedge dt, \tag{8}$$

with $B_k^i = \varepsilon_{kpq}\big(\partial_p A_q^i + \frac{1}{2}\varepsilon_{ilm}A_p^l A_q^m\big)$ referred to as the swirl intensity and $H_k^i = \partial_k \Phi^i - \partial_t A_k^i + \varepsilon_{ilm}A_k^l \Phi^m$ the micro–eddy intensity. From (8), the structural equations, mathematically called the Bianchi identity, can be derived as

$$D\mathbf{F}^i = d\mathbf{F}^i + \varepsilon_{ijk}\mathbf{W}^j \wedge \mathbf{F}^k \equiv \mathbf{0}. \tag{9}$$

Geometrically, the vortex fields consist of 12 components, but an arbitrary transformation of frame with 3 parameters is permitted (see Section 4), that is to say, only 9 variables in the vortex fields are objective for the description of structures on the manifolds, while the derived curvature tensor is objective, whose 18 components need 9 identities as given by (9) to restrict.

In summary, the flow fields and their intensities can be explained in terms of the element as

- ✧ v_i: velocity or the displacement of an element after unit time;
- ✧ $Y_{ki} = D_k v_i = \partial_k v_i + \varepsilon_{ilm}A_k^l v_m$: the difference of displacement of the element after unit time when translating unit distance along the direction $\mathbf{e}_k$;
- ✧ Φ^i: the left micro–rotation in the element after unit time;
- ✧ A_k^i: the required micro–rotation of the element when translating unit distance along the direction $\mathbf{e}_k$;
- ✧ B_k^i: the micro–rotation jump of the element when translating along a loop with unit area perpendicular to $\boldsymbol{e}_k$;

✧ H_k^i: the difference of left micro–rotation in the element after unit time and when translating unit distance along the direction $\mathbf{e}_k$.

From another view of point, the flow fields are the average (statistical) properties of a large number of particulates in the element, and so must be transportable during the microscopic diffusion of particulates. This results in the coupling of the velocity and the vortex fields. As mentioned above, a particulate with velocity v_i diffusing unit distance along the direction $\mathbf{e}_k$ (or across the unit area perpendicular to $\mathbf{e}_k$) will transport a momentum $\partial_k v_i$ plus an increment $\varepsilon_{ilm}A_k^l v_m$ induced by the ordering atmosphere. The processes of a group of particulates yield the expression (6) of slip friction. Mathematically, it is simply a replacement of the ordinal differential by the covariant differential considering the connection. A further and marvelous contribution of microscopic diffusion

$$\boldsymbol{\chi}_i = DD\mathbf{u}_i = \varepsilon_{ilm}B_k^l v_m \, da_k \wedge dt \tag{10}$$

indicates the induced jump of momentum $\chi_{ki} = \varepsilon_{ilm}B_k^l v_m$ emerging from the ordering structure when a particulate diffusing along a loop with unit area perpendicular to $\mathbf{e}_k$. Besides, the micro–eddy indicated by Φ^i is rather different from the global translation represented by v_i. The former may be understood as the disorder during the ordering adjustment of particulates, though it actually opens a new way to intervene in the main stream. Thus, the micro–eddy intensity H_k^i can be understood as the flux of micro-rotation per time carried by the particulates diffusing unit distance along the direction $\mathbf{e}_k$.

3. Viscous Interactions Under Ordering Atmosphere

The vortex fields, indicating the shear-induced ordering (Figure 2) and as the active memory of flow history, strongly interact with the microscopic diffusion of particulates, such that some complicated structures and mechanism could emerge from this atmosphere. According to the simplified model of the new theory, the global rigid-body rotation of a bulk of fluid, say the micro–finite element, cannot come true through viscosity interaction.

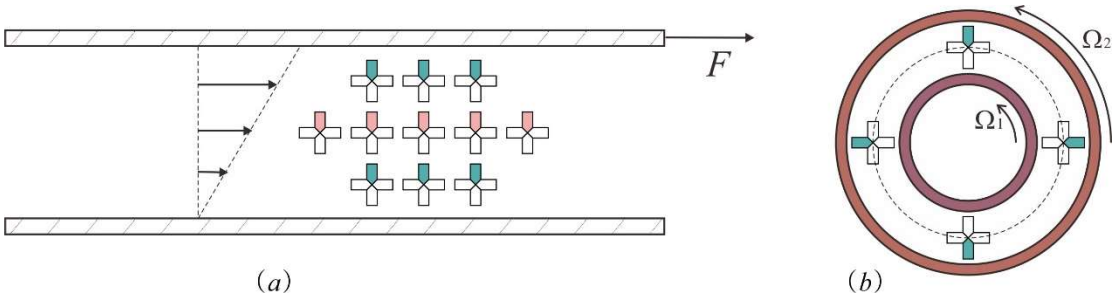


Figure 2. Shear-induced ordering: the particulates at different places are statistically considered as the same after (**a**) simple translation when flow is straight, (**b**) translation and rotation when flow is curved.

The viscous interaction working under the ordering atmosphere has become diverse. Besides those activated by the microscopic diffusion of particulates, the twirling process to bind the main stream and slip friction is indicated by $J_k^i = \varepsilon_{ilm}\sigma_{kl}v_m$, which makes sense when the direction of shear deviates from the direction of flow. It is believable that the twirling mechanism coming from the non–parallelism of shear and flow would be an important origin of the complexity of turbulence. The twirling interaction is usually indicated by an axial vector 3-form $J_k^i da_k \wedge dt$ with the measure of moment of force.

From the above discussion, we can conclude that the swirl field joins the viscous interaction by coupling with the velocity, while the micro–eddy field will form an independent kind of viscous interaction. As the general routine to construct a physical theory, the variational principle from the Lagrangian density of the fluid is expectable. The merits of a variational derived theory include a certain internal consistency, the fact that the physical symmetries of the system can be directly related to conservation laws that are

satisfied by any and all solutions, and last but not least, the fact that variational formulations lead to a complete theory of compatible boundary and initial data. For instance, the Lagrangian density

$$L_{Eu}[v_i] = v_i(\rho a_i - f_i + \partial_i p) \tag{11}$$

can be used to obtain the Euler equations

$$M_i = \frac{\partial L_{Eu}}{\partial v_i} = \rho a_i - \rho f_i + \partial_i p = 0, \tag{12}$$

for perfect and incompressible fluids, where the acceleration a_i, body force f_i and pressure p should be regarded as invariant in the variational process. For real fluids with viscosity, an additional Lagrangian density L_{vis} can be constructed as

$$L_{vis}\left[v_i, W_\mu^j\right] = L_Y[Y_{ki}] + L_\chi[\chi_{ki}] - L_\Phi\left[\Phi^i\right] - L_H\left[H_k^i\right] \tag{13}$$

following the minimal replacement and the minimal coupling principles of the gauge field theory (cf. [10]), where L_Y, L_χ, L_Φ, L_H are non–negative energy functionals of generalized fluxes $Y_{ki}, \chi_{ki}, \Phi^i, H_k^i$. In the above formulation, the micro–eddy field represents a motion with micro-scale and essentially dissipative, which is independent to the main stream. The minus signs in front of L_Φ and L_H proclaim the transferability of the action quantities between the micro–eddies and the main stream, through the viscous interactions and with the swirl structures as a bridge. Based on the Lagrangian density

$$L\left[v_i, W_\mu^j\right] = L_{Eu}[v_i] + L_{vis}\left[v_i, W_\mu^j\right], \tag{14}$$

we list the work conjugate pairs of generalized fluxes and forces in Table 1, where some relations between the generalized forces and the generalized fluxes can be regarded as constitutive laws, while the others are just derived through the coupling processes, say $\Sigma_i = \frac{\partial L_Y}{\partial v_i} = \varepsilon_{ilm} B_k^m \frac{\partial L_Y}{\partial \chi_{kl}}$.

Table 1. Work conjugate pairs of generalized fluxes and forces in viscous interactions.

Generalized Fluxes	Generalized Forces	Property
v_i	$\Sigma_i = \frac{\partial L_Y}{\partial v_i} = \varepsilon_{ilm}\Pi_{kl}B_k^m$	Coupling, vector bulk space–time 4–form
Φ^i	$m^i = \frac{\partial L_\Phi}{\partial \Phi^i}$	Constitutive, axial vector bulk 3–form
A_k^i	$J_k^i = -\frac{\partial L_Y}{\partial A_k^i} = \varepsilon_{ilm}\sigma_{kl}v_m$	Coupling, axial vector space–time 3–form
$Y_{ki} = \partial_k v_i + \varepsilon_{ilm}A_k^l v_m$	$\sigma_{ki} = \frac{\partial L_Y}{\partial Y_{ki}}$	Constitutive, vector area space–time 3–form
$\chi_{ki} = \varepsilon_{ilm}B_k^l v_m$	$\Pi_{ki} = \frac{\partial L_\chi}{\partial \chi_{ki}}$	Constitutive, vector space–time 2–form
$H_k^i = \partial_k \Phi^i - \partial_t A_k^i + \varepsilon_{ilm}A_k^l \Phi^m$	$E_k^i = \frac{\partial L_H}{\partial H_k^i}$	Constitutive, axial vector area 2–form
$B_k^i = \varepsilon_{kpq}\left(\partial_p A_q^i + \frac{1}{2}\varepsilon_{ilm}A_p^l A_q^m\right)$	$G_k^i = \frac{\partial L_\chi}{\partial B_k^i} = \varepsilon_{ilm}v_l\Pi_{km}$	Coupling, axial vector space–time 2–form

4. Dynamical Equations of Viscous Flow

Use φ_i, η_k^i and η_4^i as the variations of v_i, A_k^i and Φ^i, respectively, namely

$$\varphi_i = \delta v_i, \eta_k^i = \delta A_k^i, \eta_4^i = \delta \Phi^i,$$

so from

$$\delta Y_{ki} = \partial_k \varphi_i + \varepsilon_{ilm}A_k^l \varphi_m + \varepsilon_{ilm}\eta_k^l v_m,$$

$$\delta B_k^i = \varepsilon_{kpq}\left(\partial_p \eta_q^i + \varepsilon_{ilm}\eta_p^l A_q^m\right),$$

$$\delta H_k^i = \partial_k \eta_4^i - \partial_t \eta_k^i + \varepsilon_{ilm}\eta_k^l \Phi^m + \varepsilon_{ilm} A_k^l \eta_4^m,$$

we have the variation of the Lagrangian density respect to $\{v_i, W_\mu^j\}$ as

$$\begin{aligned}\delta L &= (M_i + \Sigma_i)\varphi_i + \sigma_{ki}\delta Y_{ki} - m^i \eta_4^i + G_k^i \delta B_k^i - E_k^i \delta H_k^i \\ &= \left(M_i + \Sigma_i - \partial_k \sigma_{ki} - \varepsilon_{ilm} A_k^l \sigma_{km}\right)\varphi_i + \partial_k(\sigma_{ki}\varphi_i) \\ &\quad -\left(m^i - \partial_k E_k^i - \varepsilon_{ilm} A_k^l E_k^m\right)\eta_4^i - \partial_k\left(E_k^i \eta_4^i\right) \\ &\quad -\left[J_k^i + \partial_t E_k^i + \varepsilon_{ilm}\Phi^l E_k^m - \varepsilon_{kpq}\left(\partial_p G_q^i + \varepsilon_{ilm} A_p^l G_q^m\right)\right]\eta_k^i \\ &\quad + \partial_t\left(E_k^i \eta_k^i\right) - \partial_k\left(\varepsilon_{kpq} E_p^i \eta_q^i\right).\end{aligned}$$

Thus, noticing that the variations of field variables are independent to each other and vanish on the boundary, the minimal action principle of the fluid system on the space–time domain $\mathcal{D}$ the fluid occupies

$$\delta \int_{\mathcal{D}} L\left[v_i; A_k^i, \Phi^i\right] dv \wedge dt = \int_{\mathcal{D}} \delta L\left[v_i; A_k^i, \Phi^i\right] dv \wedge dt = 0, \tag{15}$$

finally yields the dynamical relations between the generalized forces, which can be compactly written with the differential forms as

$$\mathbf{M}_i + \mathbf{\Sigma}_i = d\boldsymbol{\sigma}_i + \varepsilon_{ilm}\mathbf{A}^l \wedge \boldsymbol{\sigma}_m = D\boldsymbol{\sigma}_i, \tag{16}$$

$$\mathbf{J}^i = d\mathbf{Q}^i + \varepsilon_{ilm}\mathbf{W}^l \wedge \mathbf{Q}^m = D\mathbf{Q}^i, \tag{17}$$

where

$$\mathbf{J}^i = \frac{\partial L_\Phi}{\partial \Phi^i} dv - \frac{\partial L_Y}{\partial A_k^i} da_k \wedge dt = \mathbf{m}^i + \varepsilon_{ilm}\boldsymbol{\sigma}_l \wedge \mathbf{u}_m, \mathbf{Q}^i = \frac{\partial L_H}{\partial H_k^i} da_k - \frac{\partial L_\chi}{\partial B_k^i} dx_k \wedge dt = \mathbf{E}^i + \varepsilon_{ilm}\mathbf{\Pi}_l \wedge \mathbf{u}_m, \tag{18}$$

besides the generalized fluxes/forces defined in Table 1.

It should be pointed out that the exterior differentials (16) are confined to be of spatial, since the force equilibrium holds on any volume domain at every instant. But in (17), there are two parts: one is about the micro–moments of force over the volume domain, another is about the micro–moment fluxes of force across the surface domain. It is interesting that since the two parts of micro–moments of force are not completely independent, the derived integrability condition of (17)

$$D\mathbf{J}^i = d\mathbf{J}^i + \varepsilon_{ilm}\mathbf{W}^l \wedge \mathbf{J}^m = \varepsilon_{ilm}\mathbf{F}^l \wedge \mathbf{Q}^m = \varepsilon_{ilm}\left(H_k^l E_k^m + B_k^l G_k^m\right) dv \wedge dt \tag{19}$$

is usually simplified to covariant conservation of the micro–moment current

$$D\mathbf{J}^i \equiv 0 \tag{20}$$

if the coaxialities between **H** and **E**, **B** and **G** are satisfied, respectively. By virtue of the coaxialities between **m** and **Φ**, **σ** and **Y**, further expansion of (20) yields

$$\partial_t m^i = \varepsilon_{ilm} v_l D_k \sigma_{km} \tag{21}$$

implying that the bulk twirling interaction directly produces the micro-eddies.

Different fluids may possess different constitutive laws and different properties of matter. For most fluids consisting of small molecules, the intrinsic isotropy will guarantee the coaxiality between the generalized fluxes and forces in the constitutive laws. Further, for the Newton's fluids, like water and air in ordinary flows [11], the Lagrangian density is simply quadratic, such that

$$L\left[v_i, W_\mu^j\right] = (\rho a_i - \rho f_i + \partial_i p)v_i + \frac{1}{2}\mu\left(Y_{ki}Y_{ki} - \Phi^i\Phi^i\right) + \frac{1}{2}\mu\Lambda(\chi_{ki}\chi_{ki} - H_k^i H_k^i) \tag{22}$$

contains only two parameters of matter: the familiar viscosity coefficient μ and a new parameter Λ with the dimension of area, which could be related to the size of a micro–finite element. Under the construction (22) of Lagrangian density, which is equivalent to providing a specific generalized flow/force relationship including all constitutive relationships, the dynamical Equations (16) and (17) can be expanded to obtain the following control equations of incompressible flow fields

$$\rho\frac{dv_i}{dt} - \rho f_i + \partial_i p = \mu\nabla^2 v_i + \mu\varepsilon_{ilm}\left(2A_k^l\partial_k v_m + v_m\partial_k A_k^l\right) - \mu h_{ij,mn}(A_k^m A_k^n + \Lambda B_k^m B_k^n)v_j, \tag{23}$$

$$\mu\Phi^i = \mu\Lambda\left(\partial_k H_k^i + \varepsilon_{ilm}A_k^l H_k^m\right), \tag{24}$$

$$\mu\varepsilon_{ilm}v_l Y_{km} = \mu\Lambda\left(\partial_t H_k^i + \varepsilon_{ilm}\Phi^l H_k^m\right) - \mu\Lambda\varepsilon_{kpq}\left[\partial_p\left(h_{ir,st}v_s v_t B_q^r\right) + \varepsilon_{ilm}A_p^l h_{mr,st}v_s v_t B_q^r\right] \tag{25}$$

for the velocity, micro–eddy and swirl fields, respectively, where the viscosity coefficient μ in (24) and (25) can be eliminated from both sides, and

$$h_{ij,mn} \triangleq \varepsilon_{kim}\varepsilon_{kjn} = \delta_{ij}\varepsilon_{mn} - \delta_{in}\varepsilon_{jm}. \tag{26}$$

As mentioned above, these equations represent the balances of momentum and micro–moments in fluid. The Equations (23)–(25) together with the continuity equation $\partial_k v_k = 0$ constitute a close system of sixteen equations for the sixteen field quantities $\left\{p, v_i, A_k^i, \Phi^i\right\}$. Finally, it is easy to verify that the conservation relation (21) of micro–moment current takes the form

$$\partial_t\Phi^i = \varepsilon_{ilm}v_l D_k Y_{km} \tag{27}$$

seeming to be a geometrical relation without any property of matter.

5. Preliminary Analyses of the Dynamical Equation

5.1. Energy Equilibriums

Rewrite the dynamical Equations (16) and (17) in the component form, namely

$$\rho a_i - \rho f_i + \partial_i p + \Sigma_i = \partial_k\sigma_{ki} + \varepsilon_{ilm}A_k^l\sigma_{km}, \tag{28}$$

$$m^i = \partial_k E_k^i + \varepsilon_{ilm}A_k^l E_k^m, \tag{29}$$

$$\varepsilon_{ilm}v_l\sigma_{km} = \partial_t E_k^i + \varepsilon_{ilm}\Phi^l E_k^m - \varepsilon_{kpq}\left(\partial_p G_q^i + \varepsilon_{ilm}A_p^l G_q^m\right), \tag{30}$$

we can derive the equilibrium equations

$$\rho a_i v_i - \rho f_i v_i + v_i\partial_i p + \Sigma_i v_i = \partial_k(\sigma_{ki}v_i) - \sigma_{ki}Y_{ki}, \tag{31}$$

$$m^i\Phi^i = \partial_k\left(E_k^i\Phi^i\right) - E_k^i\partial_t A_k^i - E_k^i H_k^i, \tag{32}$$

$$\varepsilon_{ilm}A_k^i v_l\sigma_{km} = \partial_t\left(E_k^i A_k^i\right) - E_k^i\partial_t\Phi^i + E_k^i H_k^i - \varepsilon_{kpq}\partial_p\left(A_k^i G_q^i\right) - G_k^i B_k^i - \frac{1}{2}\varepsilon_{kpq}\varepsilon_{ilm}A_p^l A_q^m G_k^i. \tag{33}$$

From the first two equations, we find the non-negative dissipative terms $\sigma_{ki}Y_{ki}, \Sigma_i v_i$ and $E_k^i H_k^i$, and the boundary acting terms $\partial_k(\sigma_{ki}v_i)$ and $\partial_k\left(E_k^i\Phi^i\right)$; it is interesting that there appears a term $E_k^i\partial_t A_k^i$ from the changing of the swirl field in (32), transferring energy between the structures and micro–eddies through the changing of the swirl field. The third equation is of the energy transfer: two non–negative terms $E_k^i H_k^i$ and $G_k^i B_k^i$, having different signs here, indicates the exchange of energy between the swirl structures and the micro-eddies; the term $\partial_t\left(E_k^i A_k^i\right)$ can be regarded as the increase of energy stored in the swirl field,

while the term $\varepsilon_{ilm}A_k^i v_l \sigma_{km}$ shows the contribution of the twirling process from the mainstream. The combination of the three energy equations results in the equilibrium of total mechanical energy as

$$\begin{aligned}\frac{d}{dt}\left(\frac{\rho v_i v_i}{2}\right) + \sigma_{ki}Y_{ki} + m^i\Phi^i + E_k^i H_k^i \\ = f_i v_i + \partial_i(pv_i) + \partial_k(\sigma_{ki}v_i) + \partial_k\left(E_k^i\Phi^i\right) - \partial_t\left(E_k^i A_k^i\right) + \varepsilon_{kpq}\partial_p\left(A_k^i G_q^i\right) \\ + \varepsilon_{ilm}A_k^i v_l \sigma_{km} + \varepsilon_{ilm}\Phi^l A_k^m E_k^i + \frac{1}{2}\varepsilon_{kpq}\varepsilon_{ilm}A_p^l A_q^m G_k^i,\end{aligned} \tag{34}$$

where uses are made of the continuity equation $\partial_k v_k = 0$ and $G_k^i B_k^i = \Sigma_i v_i$. The increase of kinetic energy and the dissipative terms are listed in the left, while besides the works of body force, pressure, and boundary viscous forces, the right includes three terms which can be understood as the coupling works of different fields.

5.2. Field Equations Under Frenet Frames of Instant Streamlines

A streamline at the instant *t* and across the point $\mathbf{r}_0$ is a one–parameter space curve defined by

$$\frac{d\mathbf{r}(\tau;t)}{d\tau} = \mathbf{v}(\mathbf{r},t) = V\mathbf{n}, \mathbf{r}(0;t) = \mathbf{r}_0, \tag{35}$$

where $V \geq 0$ is the speed, and the unit vector $\mathbf{n}$ indicates the direction of flow. The streamline at a point with non–zero speed is unique and independent of the speed. The following discussion in this paper will not consider zero velocity points for now, as in most flows, the number of zero velocity points is zero or very small. Thus we can rewrite the streamline equation as

$$\frac{d\mathbf{r}(s;t)}{ds} = \mathbf{n}(\mathbf{r},t), \mathbf{r}(0;t) = \mathbf{r}_0, \tag{36}$$

where the one-parameter is the arc length of the streamline starting from $\mathbf{r}_0$.

According to differential geometry, the characteristic of the streamline as a space curve can be determined by the arc length *s*, the curvature κ and torsion ϖ (if the curvature is non–zero) within a rigid motion (a translation plus a rotation). Denote by

$$\partial_n = \mathbf{n}\cdot\nabla, \tag{37}$$

we have the relations of the Frénet (orthogonal) frame $\{\boldsymbol{\xi}_1, \boldsymbol{\xi}_2, \boldsymbol{\xi}_3\}$ as

$$\boldsymbol{\xi}_3 = \mathbf{n}, \partial_n\boldsymbol{\xi}_3 = \kappa\boldsymbol{\xi}_1, \partial_n\boldsymbol{\xi}_1 = -\kappa\boldsymbol{\xi}_3 + \varpi\boldsymbol{\xi}_2, \partial_n\boldsymbol{\xi}_2 = -\varpi\boldsymbol{\xi}_1. \tag{38}$$

Assume that

$$\boldsymbol{\xi}_i = R_{ij}\mathbf{e}_j, \tag{39}$$

using the definition

$$D\boldsymbol{\xi}_i = \varepsilon_{ijk}\widetilde{\mathbf{W}}^j\boldsymbol{\xi}_k, \tag{40}$$

we can derive the connection and the curvature tensor under the Frénet frames as

$$\widetilde{\mathbf{W}}^i = R_{ij}\mathbf{W}^j - \mathbf{w}^j, \tilde{\mathbf{F}}^i = D\widetilde{\mathbf{W}}^i = R_{ij}\mathbf{F}^j, \tag{41}$$

with

$$\mathbf{w}^i = \frac{1}{2}\varepsilon_{ilm}R_{lk}dR_{mk}. \tag{42}$$

The transformation relations (41) show that the curvature tensor is a tensor that changes covariantly with the frame, whereas the connection is not. It is remarkable that all terms after covariant differential are covariant, for instance, we have the transformations of the generalized fluxes $\mathbf{Y}_i$ and $\boldsymbol{\chi}_i$ as

$$\widetilde{\mathbf{Y}}_i = R_{ij}\mathbf{Y}_j, \widetilde{\boldsymbol{\chi}}_i = R_{ij}\boldsymbol{\chi}_j. \tag{43}$$

As for the quantities M_i and m^i, there exist a kinematic explanation to guarantee their covariance, namely, the missing acceleration and micro–eddy observed in the space-time inhomogeneous frame must be picked up in the dynamical equilibriums. Therefore, the dynamical equations possess the form invariance as

$$\rho(\tilde{a}_i + \varepsilon_{il3}\Omega^l V) - \rho\tilde{f}_i + \tilde{\partial}_i p + \tilde{\Sigma}_i = \partial_k\tilde{\sigma}_{ki} + \varepsilon_{ilm}\tilde{A}_k^l\tilde{\sigma}_{km}, \tag{44}$$

$$\tilde{m}^i = \partial_k\tilde{E}_k^i + \varepsilon_{ilm}\tilde{A}_k^l\tilde{E}_k^m, \tag{45}$$

$$\varepsilon_{i3m}V\tilde{\sigma}_{km} = \partial_t\tilde{E}_k^i + \varepsilon_{ilm}\widetilde{\Phi}^l\tilde{E}_k^m - \varepsilon_{kpq}\left(\partial_p\tilde{G}_q^i + \varepsilon_{ilm}\tilde{A}_p^l\tilde{G}_q^m\right), \tag{46}$$

where

$$\Omega^3 = 0;\ \Omega^i = \varepsilon_{li3}R_{lm}\frac{dR_{3m}}{dt} = -w_4^i - v_k w_k^i = -w_4^i - \kappa V\delta_{i1}, i \neq 3 \tag{47}$$

coming from the relation

$$\tilde{a}_i + \varepsilon_{il3}\Omega^l V = R_{ij}\frac{dv_j}{dt} = \delta_{i3}\frac{dV}{dt} + VR_{ij}\frac{dR_{3j}}{dt}. \tag{48}$$

For the Newtonian fluids defined by the Lagrangian density (22), the field equations become

$$\delta_{i3}\frac{dV}{dt} + \varepsilon_{il3}V\Omega^l - \tilde{f}_i + \tilde{\partial}_i\frac{p}{\rho} = \nu\delta_{i3}\nabla^2 V + \nu\varepsilon_{il3}\left(2\tilde{A}_k^l\partial_k V + V\partial_k\tilde{A}_k^l\right) - \nu h_{i3,mn}\left(\tilde{A}_k^m\tilde{A}_k^n + \Lambda\tilde{B}_k^m\tilde{B}_k^n\right)V, \tag{49}$$

$$\widetilde{\Phi}^i + w_4^i = \Lambda\left(\partial_k\widetilde{H}_k^i + \varepsilon_{ilm}\tilde{A}_k^l\widetilde{H}_k^m\right), \tag{50}$$

$$V^2\left(\tilde{A}_k^i - \delta_{i3}\tilde{A}_k^1\right) = \Lambda\left(\partial_t\widetilde{H}_k^i + \varepsilon_{ilm}\widetilde{\Phi}^l\widetilde{H}_k^m\right) - \Lambda\varepsilon_{kpq}\left\{\partial_p\left[V^2\left(\tilde{B}_q^i - \delta_{i3}\tilde{B}_q^3\right)\right] + \varepsilon_{ilm}\tilde{A}_p^l V^2\left(\tilde{B}_q^m - \delta_{m3}\tilde{B}_q^3\right)\right\}, \tag{51}$$

where ν is the kinematical viscosity of fluid.

The conservation relation (27) under the Frénet frame becomes

$$\partial_t\left(\widetilde{\Phi}^i + w_4^i\right) + \varepsilon_{ilm}\widetilde{\Phi}^l\widetilde{w}_4^m = \partial_k\left[V^2\left(\tilde{A}_k^i - \delta_{i3}\tilde{A}_k^3\right)\right] + \varepsilon_{i3m}V^2\tilde{A}_k^3\tilde{A}_k^m. \tag{52}$$

The streamwise projections of Equations (49), (51) and (52), namely

$$\frac{dV}{dt} - \tilde{f}_3 + \tilde{\partial}_3\frac{p}{\rho} = \nu\nabla^2 V - \nu\left(\tilde{A}_k^1\tilde{A}_k^1 + \tilde{A}_k^2\tilde{A}_k^2 + \Lambda\tilde{B}_k^1\tilde{B}_k^1 + \Lambda\tilde{B}_k^2\tilde{B}_k^2\right)V, \tag{53}$$

$$0 = \partial_t\widetilde{H}_k^3 + \varepsilon_{lm3}\widetilde{\Phi}^l\widetilde{H}_k^m - \varepsilon_{kpq}\varepsilon_{lm3}V^2\tilde{A}_p^l\tilde{B}_q^m, \tag{54}$$

$$\partial_t\left(\widetilde{\Phi}^3 + w_4^3\right) + \varepsilon_{lm3}\widetilde{\Phi}^l\widetilde{w}_4^m = 0 \tag{55}$$

reveal the following information: (i) the flow has a resistance proportional to the speed if there are swirl structures perpendicular to the flow, (ii) the origin of the streamwise vortex fields is completely geometrical, namely from the non-interchangeability of the rotation group. Their projections of Equations (49), (51), and (52) to the direction perpendicular to the main stream yield ($i \neq 3$)

$$V\Omega^i + \varepsilon_{il3}\tilde{f}_l - \varepsilon_{il3}\rho^{-1}\tilde{\partial}_l p = \nu V^{-1}\partial_k\left(V^2\tilde{A}_k^i\right) - \nu\varepsilon_{il3}\left(\tilde{A}_k^l\tilde{A}_k^3 + \Lambda\tilde{B}_k^l\tilde{B}_k^3\right)V, \tag{56}$$

$$V^2\tilde{A}_k^i = \Lambda\left(\partial_t\widetilde{H}_k^i + \varepsilon_{ilm}\widetilde{\Phi}^l\widetilde{H}_k^m\right) - \Lambda\varepsilon_{kpq}\left[\partial_p\left(V^2\tilde{B}_q^i\right) - \varepsilon_{il3}V^2\tilde{A}_p^3\tilde{B}_q^l\right], \tag{57}$$

$$\partial_t\left(\widetilde{\Phi}^i + w_4^i\right) + \varepsilon_{ilm}\widetilde{\Phi}^l\widetilde{w}_4^m = \partial_k\left(V^2\tilde{A}_k^i\right) - \varepsilon_{il1}V^2\tilde{A}_k^3\tilde{A}_k^l. \tag{58}$$

The combination of (56) and (58)

$$\nu\partial_t\left(\widetilde{\Phi}^i + w_4^i\right) + \nu\varepsilon_{ilm}\widetilde{\Phi}^l\widetilde{w}_4^m = \left(V\Omega^i + \varepsilon_{il3}\tilde{f}_l - \varepsilon_{il3}\rho^{-1}\tilde{\partial}_l p\right)V + \nu\varepsilon_{il3}\Lambda\tilde{B}_k^l\tilde{B}_k^3V^2, i \neq 3 \tag{59}$$

shows that the generation of non–streamwise micro–eddies may come from the non–parallelism between the resultant force of non–viscous force and stream, or the coupling of the swirl intensity along different directions.

5.3. Expansions of Field Equations According to Master Variables and Their One-Dimensional Models

All field Equations (23)–(25) can be written in a four-term standard form according to their master variables as

$$\text{Unsteady term} + \text{Linear term} + \text{Diffusion term} = \text{Source term}. \tag{60}$$

In order to express the expansions of field equations in a compact form as possible, we introduce the following notations: (i) maintain all terms in the velocity equations if they are the same as in the classical theory; (ii) keep their original expression if they obviously include no master variable, (iii) for a free index i, use (i, i_1, i_2) as an even permutation of $(1,2,3)$, for example (i, i_1, i_2) corresponds to $(2,3,1)$ if $i = 2$, the sum for repeated Greek alphabet, say α in i_α, is from $\alpha = 1$ to 2, (iv) use $\langle i_1, i_2\rangle$ for the sum in an asymmetrical way, for example

$$\Phi^{\langle j_1}\partial_t A_k^{j_2\rangle} = \Phi^{j_1}\partial_t A_k^{j_2} - \Phi^{j_2}\partial_t A_k^{j_1}, \tag{61}$$

and (v) for the repeated indices with underscore, the sum convention no longer works. Then, from (23)–(25), after some lengthy derivations, we obtain the most detailed expanded equations of the controlling fields $\{v_i, \Phi^i, A_k^i\}$

$$\frac{dv_i}{dt} + \nu\left(A_k^{i_\alpha}A_k^{i_\alpha} + \Lambda B_k^{i_\alpha}B_k^{i_\alpha}\right)v_i - \nu\nabla^2 v_i = f_i - \partial_i\left(\frac{p}{\rho}\right) + \nu\left(2A_k^{\langle i_1}\partial_k v_{i_2\rangle} - v_{\langle i_1}\partial_k A_k^{i_2\rangle}\right) + \nu\left(A_k^i A_k^{i_\alpha} + \Lambda B_k^i B_k^{i_\alpha}\right)v_{i_s}, \tag{62}$$

$$\left(\Lambda^{-1} + A_k^{i_\alpha}A_k^{i_\alpha}\right)\Phi^i - \nabla^2\Phi^i = A_k^{i_\alpha}\Phi^{i_\alpha}A_k^i - \partial_t\partial_k A_k^i + 2A_k^{\langle i_1}\partial_k\Phi^{i_2\rangle} - A_k^{\langle i_1}\partial_t A_k^{i_2\rangle} - \Phi^{\langle i_1}\partial_k A_k^{i_2\rangle}, \tag{63}$$

$$\begin{aligned}
&\partial_t\partial_t A_k^i + \left[\Lambda^{-1}v_{i_\alpha}v_{i_\alpha} - \Phi^{i_\alpha}\Phi^{i_\alpha} + v_{\underline{i}}v_{\underline{i}}A_{k_\beta}^{i_\alpha}A_{k_\beta}^{i_\alpha} + v_{i_\alpha}v_{i_s}A_{k_\beta}^{i_\alpha}A_{k_\beta}^{i_s} + \partial_{k_\beta}\left(v_i v_{\langle i_1}A_{k_\beta}^{i_2\rangle}\right)\right]A_k^i - \partial_{k_\beta}\left(v_{i_\alpha}v_{i_\alpha}\partial_{k_\beta}A_k^i\right)\\
&\quad = \Lambda^{-1}\left(v_{i_\alpha}A_k^{i_\alpha}v_i - v_{\langle i_1}\partial_k v_{i_2\rangle}\right) + \partial_t\left(\partial_k\Phi^i + A_k^{\langle i_1}\Phi^{i_2\rangle}\right) + \Phi^{\langle i_1}\left(\partial_k\Phi^{i_2\rangle} - \partial_t A_k^{i_2\rangle}\right) - \Phi^{i_\alpha}A_k^{i_\alpha}\Phi^i\\
&\quad + \partial_{k_\beta}\left[v_i v_{i_\alpha}\partial_{\langle k}A_{k_\beta\rangle}^{i_\alpha} + v_{\langle i_1}A_k^{i_2\rangle}v_{\underline{i}}A_{k_\beta}^{\underline{i}} - v_{i_\alpha}v_{i_\alpha}\left(\partial_k A_{k_\beta}^i + A_k^{\langle i_1}A_{k_\beta}^{i_2\rangle}\right)\right] + V^2A_{k_\beta}^{\langle i_1}\partial_{\langle k_\beta}A_{k\rangle}^{i_2\rangle}\\
&\quad + v_{\langle i_1}A_{k_\beta}^{i_2\rangle}v_{i_\alpha}\partial_{\langle k_\beta}A_{k\rangle}^{i_\alpha} - v_{\langle i_1}A_{k_\beta}^{i_2\rangle}v_{\underline{i}}\partial_k A_{k_\beta}^{\underline{i}} + \left(v_{\underline{i}}v_{\underline{i}}A_k^{i_\alpha}A_{k_\beta}^{i_\alpha} + v_{i_\alpha}v_{i_\beta}A_k^{i_\alpha}A_{k_\beta}^{i_\beta}\right)A_{k_\beta}^{\underline{i}} + A_{k_\beta}^{\langle i_1}v_{i_2\rangle}A_{\langle k_\beta}^{i_1}A_{k\rangle}^{i_2}v_i
\end{aligned} \tag{64}$$

where there is no $\{v_i, \Phi^i, A_k^i\}$ appearing on the right of the equations, the complex coefficients and sources show all coupling between multi–fields and multi–components.

In view of the master variables, there is no non-linear coupling of fields themselves, since the conventional coupling in the convection term of the velocity can be ascribed to the pressure, say, in the derivation

$$\frac{dv_i}{dt} + \partial_i\left(\frac{p}{\rho}\right) = \partial_t v_i + v_k(\partial_k v_i - \partial_i v_k) + \partial_i\left(\frac{p}{\rho} + \frac{V^2}{2}\right), \tag{65}$$

The second term on the right has no coupling of the master variable with itself. Other obvious features of the controlling equations include: (i) the equations the swirl fields have a second order unsteady term while the equations of the micro–eddy fields have no unsteady term, (ii) the swirl fields diffuse transversely, (iii) the coefficients of linear terms for the fields associated with motion (velocity and micro–eddy) are non-negative while those for the fields associated with structure (swirl) are indefinite. The existence of a linear term is the key point of the new theory. The linear term could be a regulator between the temporal evolution and spatial distribution: a positive coefficient of the linear term means exponential attenuation with time

and localization in space while a negative one proclaims a wavy change in space and with time if the time derivative is two orders, or exponential increase with time if the time derivative is one order.

It is interesting to truncate the field equations to yield their one–dimensional cartoon models. We find that there are three types of models

$$\partial_t V + \nu k^2 V - \nu \partial_x \partial_x V = S_V, \tag{66}$$

$$(a^{-2} + k^2)\Phi - \partial_x \partial_x \Phi = S_\Phi, \tag{67}$$

$$\partial_t \partial_t A \pm c^2 k^2 A - c^2 \partial_x \partial_x A = S_A, \tag{68}$$

for the velocity, micro–eddy and swirl fields, respectively, where ν and a are properties of the fluid, k and c are parameters depending on the flow. These model equations can be used to discuss the evolution characteristic of different fields.

6. A Verification Experiment

For a parallel flow with linear shear, say the Couette flow between two parallel plates (Figure 2), the theory of the N–S equations admits that two pairs of shear stresses equal to each other on the surfaces force the element distort and rotate, as shown in Figure 3 (right bottom), where the scale of a fluid particle cannot be finite: the continuous distortion makes it untraceable. The theory presented in this paper tells a different story about this simple flow (Figure 3 (right top)), where the fluid layered at the molecular slip over each other, and a moving fluid element (Figure 1) with micro-finite scale should be open or cannot be regarded as the original one after any finite time. Regarding the viscous force, we want to question the existence of shear on the surface normal to the flow direction, although it does not affect the velocity distribution in straight flow conditions. However, there is no way to measure it directly.

When the streamlines are curved, the shears on the surface normal to the flow direction will produce a force component along the flow direction, which is called the bending flow effect. That is to say, the additional shear forces can change the velocity distribution in curved laminar flows, and such an effect can be used to verify the existence of these shears. Thus, in order to distinguish the slip viscosity model from the strain-rate one, we have implemented a simple Taylor–Couette (T–C) laminar flow experiment, where two concentric cylinders rotate at the same angular speed [12].

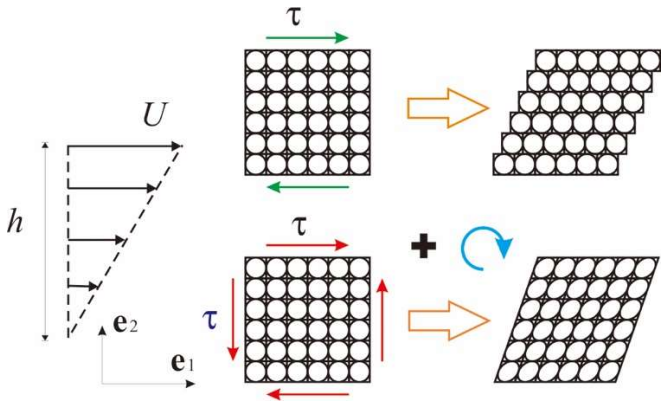


Figure 3. Different understandings of the parallel shear flow.

In general, consider the fluid flow between two concentric cylinders that are standing upright and infinitely long, with radii R_1 and R_2, and rotating around their axis with angular speeds Ω_1 and Ω_2, respectively. The fluid is assumed to be incompressible, and the flow is laminar with gravity omitted. Therefore, under the assumption that both the axis of cylinders are in the z–axis of the cylindrical coordinate system $(\boldsymbol{r}, \theta, z)$, the flow fields with properties

$$v_r = v_z = 0, v_\theta = v_\theta(r), p = p(r), \tag{69}$$

must satisfy the boundary conditions

$$v_\theta = \Omega_1 R_1, r = R_1; v_\theta = \Omega_2 R_2, r = R_2. \tag{70}$$

Without considering the shears on the surface normal to the flow direction, the streamwise balance equation can reduce to

$$\frac{1}{r}\frac{\partial}{\partial r}\left(r\frac{\partial v_\theta}{\partial r}\right) = 0, \tag{71}$$

yielding the analytic solution

$$v_\theta^{new} = \Omega_1 R_1 + (\Omega_2 R_2 - \Omega_1 R_1)\frac{\ln r - \ln R_1}{\ln R_2 - \ln R_1} \tag{72}$$

under the boundary conditions (70). It is easy to see that (72) degenerates into Newton's solution [13] $v_\theta^{new} = \Omega_1 R_1$ by setting $R_2 \to \infty$ and $\Omega_2 R_2 = \Omega_1 R_1$. The analytic solution from the N–S equations can be solved to be [11]

$$v_\theta^{N-S} = \frac{\Omega_2 R_2^2 - \Omega_1 R_1^2}{R_2^2 - R_1^2} r + \frac{\Omega_2 - \Omega_1}{R_2^{-2} - R_1^{-2}} r^{-1}, \tag{73}$$

which becomes $v_\theta^{N-S}(r) = \Omega_1 R_1^2 r^{-1}$ when $R_2 \to \infty$ and $\Omega_2 R_2^2 = \Omega_1 R_1^2$, not supporting Newton's conclusion. Smith [14] argued that "Newton mistakenly balanced the forces on the inside and outside of each thin fluid shell surrounding the body, not the torques". Rather say, the strain–rate viscosity model doesn't match Newton's original intention, and it seems that no one has considered designing an experiment to verify it. When the two cylinders rotate at the same constant angular speed, say $\Omega_1 = \Omega_2 = \Omega$ in Figure 4a, the velocity in (73) becomes

$$v_\theta^{N-S} = \Omega r, \tag{74}$$

indicating that the fluid between the cylinders incurs a rigid–body rotation, the same as the cylinders, while the new theory yields the speed of flow as

$$v_\theta^{new} = \Omega R_1 + \Omega(R_2 - R_1)\frac{\ln r - \ln R_1}{\ln R_2 - \ln R_1} \neq \Omega r. \tag{75}$$

In practice, the cylinders cannot be infinitely long, and the end-walls must appear. Careful examination (including numerical simulation) shows that the presence of the end–walls does not affect the solution of the N–S equations when the inner and outer cylinders rotate at the same angular velocity. But for the new flow model, the results with and without end–walls have to be different, especially once the end-walls appear, the flow will suddenly become three–dimensional from two–dimensional, and the analytical solution is no longer available. Will the fluid in a closed container undergo a rigid-body rotation along with the container? The answer calls for a precise experimental verification, and cannot be determined based on preconceptions instead.

Before reporting our experiment and simulation results, let's first talk about two unremarkable signs that were unintentionally revealed in previous experiments. For the case the outer cylinder is at rest and the flow between cylinders is laminar, namely $\Omega_2 = 0$, after reorganizing the torque measurements by Taylor (1935, 1936) [15–17] with the dimensionless cylinder spacing (DCS) $\eta = (R_2 - R_1)/R_1 = 0.028$, Schlichting (1979) [18] reported that the torque coefficient $C_M = 0.67 T_a^{-1}$ for the inner cylinder in terms of the Taylor number $T_a = \rho\mu^{-1}\Omega_1 R_1^2 \eta^{3/2}$, but the theoretical predictions from the velocity profile (72) and (73) are $C_M^{\text{new}} = 0.6787 T_a^{-1}$ and $C_M^{\text{N-S}} = 0.6976 T_a^{-1}$, respectively. Another sign is from the

verification experiment with LDA in the Twente Turbulent Taylor–Couette (T^3C) system [19,20]. In order to test the correction formula taking into account the refraction effects of the outer cylinder wall to two LDA beams, they performed a velocity profile measurement and two cylinders rotating at the same speed, and found that the laminar profile between the cylinders slightly deviates from the theoretical linear velocity profile within 0.6% [19] when $R_1 = 200\ \text{mm}, R_2 = 279\ \text{mm}$ $(\eta = 0.395)$ or 0.75% [20] when $R_1 = 200\ \text{mm}, R_2 = 280\ \text{mm}$ $(\eta = 0.4)$. These deviations were attributed to synthesis of system errors arising from, e.g., optical misalignment or imperfections, spatially inhomogeneous refractive index in the working fluid, or noise created by the amplification and digitalization of the optical signal, even though, according to the strain-rate model, there are no end-wall effects in these cases. But according to the new model, there is a theoretical deviation 0.86% when $\eta = 0.3$, as shown in Figure 4b.

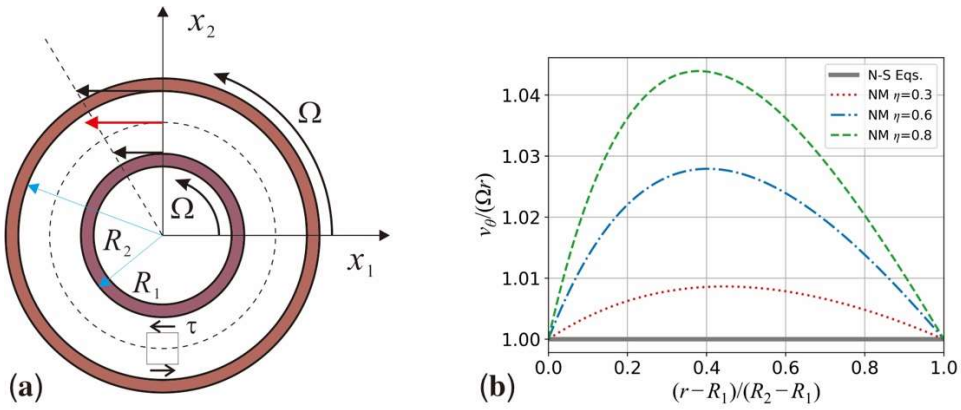


Figure 4. The scaled circumferential velocity of the new model ('NM' in the figure) and the N–S equations with different relative cylinder spacing (RCS) $\eta = (R_2 - R_1)/R_1$: (**a**) two–dimensional configuration of T–C laminar flow, (**b**) scaled velocity profile.

Since 2018, we have been committed to achieving a strict laminar-flow implementation and a precise LDA measurement of the simplest Taylor–Couette (T–C) flow, in which both the inner cylinder and the outer one are rotated at a fixed speed. The goals of our experiment are to answer (i) whether the fluid between the cylinders flow as the same as the rigid–body rotation of the cylinders, and (ii) to what extent can the end effects be eliminated to obtain the theoretically predicted two-dimensional velocity profile. Obviously, when the flow is laminar, the end-walls or even the imperfect geometry of cylinders will not impede the fluid enter into the state of rigid–body rotation according to the strain-rate viscosity mechanism; else if the physical mechanism of viscous interaction does not depend on strain-rate, the end-wall effect has to be gotten rid of by extending the length of the cylinders, and the accuracy of flow geometric boundaries must be improved as much as possible, in order to achieve the most realistic velocity profile of the designed laminar flow. The final T–C flow setup, as shown in Figure 5, includes two parts: the experimental platform and the LDA measurement system, with the schematic diagram.

The measured circumferential velocity component on the axisymmetric cross-section at the center of the two concentric cylinders rotating at the same angular velocity are obtained from 2000 consecutively samplings. To ensure laminar flow, the maximum absolute velocity of the fluid is maintained between $0.1 - 0.2\ \text{m/s}$, while the velocity signals in measurement almost present a Gaussian distribution with a stable relative standard deviation (RSD) about 0.63%. For the case $\eta = 0.3$ $(R_1 = 50\ \text{mm}, R_2 = 65\ \text{mm})$, as shown in Figure 6a,b, the maximal relative deviation from the N–S equation solution is about 0.86%, which would be misunderstood as a systematic error or within measurement error; but for the case $\eta = 0.8$ $(R_1 = 50\ \text{mm}, R_2 = 90\ \text{mm})$, as shown in Figure 6c,d, the maximal relative deviation from the theoretical solution is about 4.3%, greatly more than the RSD. The experimental results clearly do support the slip viscosity model instead of the strain–rate viscosity one [12].

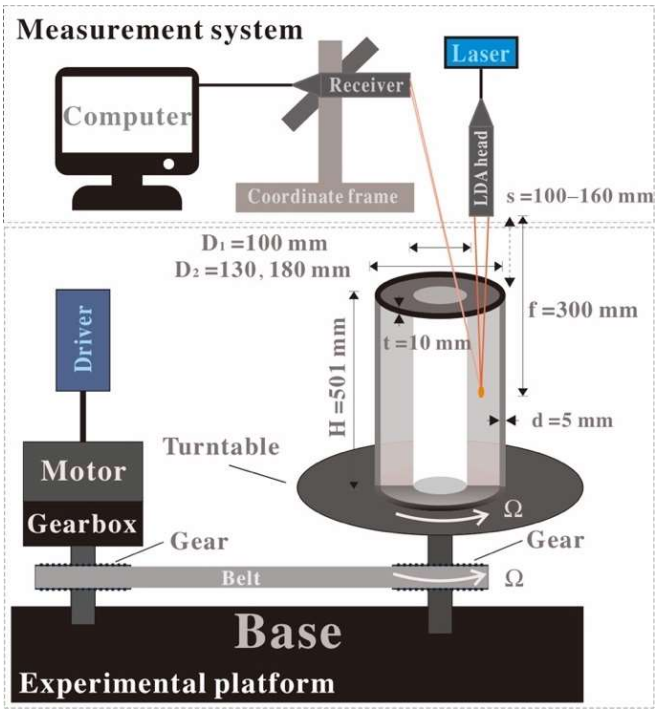
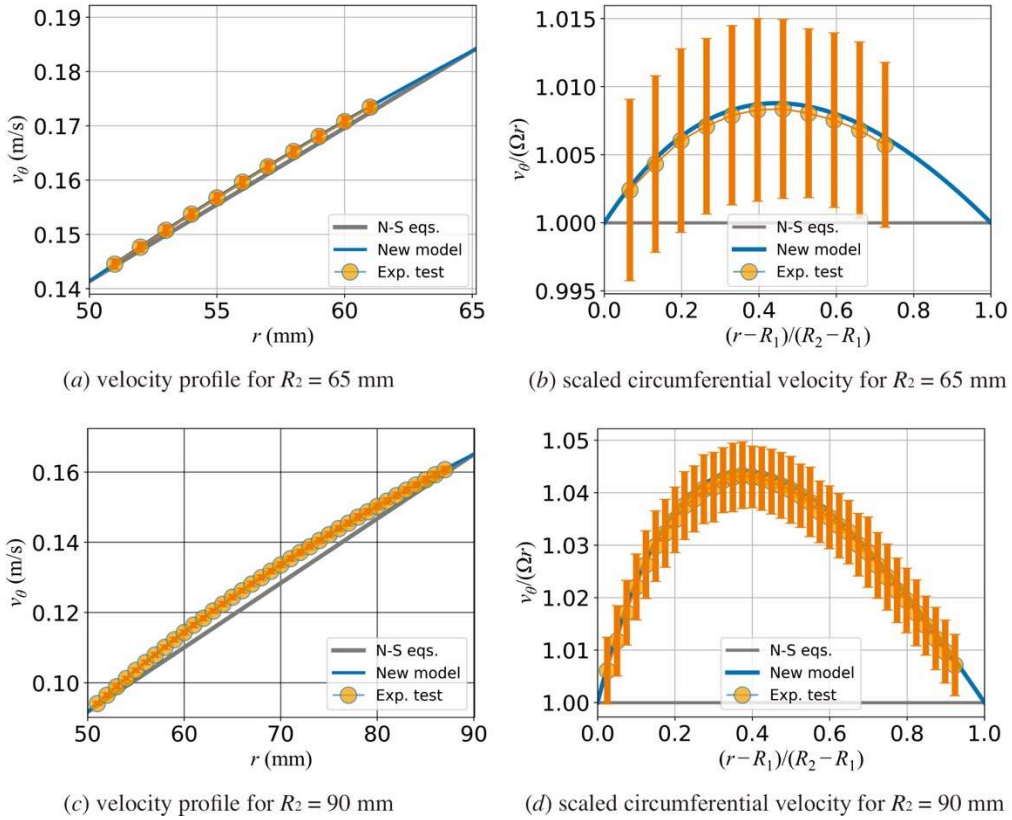


Figure 5. Schematic diagram of experimental platform and measurement system.



(*a*) velocity profile for $R_2 = 65$ mm (*b*) scaled circumferential velocity for $R_2 = 65$ mm

(*c*) velocity profile for $R_2 = 90$ mm (*d*) scaled circumferential velocity for $R_2 = 90$ mm

Figure 6. Experimental results show that the N–S equations cannot predict the velocity in the laminar T–C flow: (**a**,**c**) circumferential velocity profile and (**b**,**d**) scaled circumferential velocity for experimental parameters $R_2 = 65$ mm, $\Omega = 26.998$ rpm and $R_2 = 90$ mm, $\Omega = 17.515$ rpm, respectively.

7. Concluding Remarks

When the fluid element occupying a space-time point and endowed with the macroscopic velocity is recognized to be of micro–finite instead of infinitesimal, whatever small it is, the description of flowing as

a space–time manifold becomes natural, and the dynamics of irreversibly topological evolution of contact structures in the fluid can be constructed by expressing the viscous interaction as internal slip friction. In such a new framework, the coherent structures can be recognized through the nontrivial (non–integrable) swirl fields, and the fluid with nonzero micro–eddy can be obviously identified as the domain of turbulence with small-scale motion. The illusions of vortex pattern observed by the moving observers [18] will be clarified since the ordering structures couple with the velocity field that is uniquely determined. Therefore, the spatial pattern and the temporal dissipation are perfectly combined to a unified quantity, which can be defined as the space–time connection of the vector bundle on the manifold.

In order to compare the new flow theory proposed in this paper with the classical N–S equation theory, Tables 2 and 3 are designed based on the incompressible and linear fluids. In summary, a new theory of viscous flow is elaborated based on the micro–finite elements and the slip and twirling mechanism of viscous interactions. Unlike the corresponding theory of elasticity, here is no topologically equivalence between the theory of micro–finite element and that of the infinitesimal particle. The new variables, namely the vortex fields characterizing the structures connecting elements and the micro-eddies in the element, make the flowing fluid a space–time differential manifold covered by the micro-finite elements. Under the new description of fluid flow, the main stream, vortex structures, and micro-eddies constitute a strongly coupled system, in which nonlinear couplings between components in different directions, some of which are purely geometrical, play a critical role. When the constitutive laws are adapted to be linear, only one new property of fluid with area dimension is needed to make the controlling field equations close. Some features of fluid flow are exploited through the analyses of the derived equations. Finally, a precise T–C laminar experiment is reported to verify the rationality of the new flow theory.

Table 2. Characteristics comparing with the N–S equation theory.

Equations	**Equations (62)–(64)**	**N–S Equations**
Models	Micro-finite element + Slip viscosity	Particle + Strain-rate viscosity
Representation space of fluid	Spatiotemporal manifold	Euclidean space
Flow Field(s)	Velocity, vortex (swirl and micro-eddy)	Velocity
Framework	Minimal action principle	Newton's second law
Dynamics	Momentum, lower dimensional micro-moments (micro-moment-impulses)	Momentum, moment of momentum
Toward turbulence	Order averaging over small-scale motion	Reynold's secondary averaging

Table 3. Advantages comparing with the N–S equation theory.

Advantages	**New Flow Theory**	**N–S Equation Theory**
Can it be verified through the falsification experiment of T-C laminar flow?	✓	✕
Does the viscous force model conform to the understanding of internal friction?	✓	✕
Is the mechanism of vortex (micro torque) generation sensitive and specific?	✓	✕
Are the methods for handling multi-scale vortices reasonable and diverse?	✓	✕
Consistency between the viscosity model and the microscopic mechanism	✓	✕
Closeness for exploring turbulence	✓	✕

Acknowledgments

W.Z. acknowledges the support from Quanshui Zheng of Tsinghua University.

Ethics Statement

This work does not involve any active collection of human data, but only computer simulations of human behavior.

Informed Consent Statement

Not applicable.

Data Availability Statement

This work does not have any experimental data.

Funding

This research was funded by the NSFC (Grants No. 11372124).

Declaration of Competing Interest

The author declares that there is no conflict of interest.

Nomenclature and Key Terms

x_1, x_2, x_3	Cartesian coordinates, or spatial coordinates
$\mathbf{e}_1, \mathbf{e}_2, \mathbf{e}_3$	Cartesian bases
$t = x_4$	Time coordinate
dx_1, dx_2, dx_3, dt	Coordinate differentiations, bases of differential 1-forms
da_i, dv	Area and volume element, bases of differential 2-forms and 3-forms
$\rho, p, \mathbf{f} = f_i\mathbf{e}_i$	Density, pressure, and force of unit mass
$\mathbf{v} = v_i\mathbf{e}_i$	Macroscopic velocity field, or sections of a vector bundle, or vector field on a differentiable manifold
$V, \mathbf{n}$	Speed and velocity direction
$\mathbf{W}^i = W_4^i dx_4 + W_k^i dx_k$	Vortex field, axial-vector valued spatiotemporal differential 1-form, spatiotemporal connection on a vector bundle
$\mathbf{\Phi}^i = \Phi^i dt = W_4^i dx_4$	Micro-eddy field, temporal part of vortex field, order parameter of small-scale motion in turbulence
$\mathbf{A}^i = A_k^i dx_k = W_k^i dx_k$	Swirl field, spatial part of vortex field, representing the active slip structures of fluid layered at the molecular scale
$\delta_{ij}, \varepsilon_{ijk}$	Kronecker delta and permutation symbol
μ, ν, Λ	Kinetic viscosity, kinematic viscosity, and a new physical property parameter with area dimension
s, κ, ϖ	Arc length parameter, curvature, and torsion of a streamline
Fluid element	The smallest analytical unit for macroscopic flow of fluid, a fluid microsphere with micro-finite scale and uniquely occupying a point in the fluid domain
Macro particle	Model corresponding to a fluid element in classical flow theory, without shape and scale, with density instead of mass, a close system of fluid molecules
Ordering atmosphere	Active layered structures in flowing fluid, an internal self-organizing tension state of fluid formed during flow that can constrain molecular diffusion
Flow fields	A combination of velocity field and vortex field
Slip viscosity	New model where the viscous friction force depends on the slip strength of fluid layered at the molecular scale
Twirling interaction	Mechanism of generating viscous torque due to the non-parallelism between the viscous friction and the mainstream
Lagrangian density	For a fluid system per volume in per unit time, the increase of kinetic energy, plus viscous dissipation, minus the work done by external forces, and the dissipation due to small-scale motion

References

1. Frisch U. *Turbulence: The Legacy of A.N. Kolmogorov*; Cambridge University Press: Cambridge, UK, 1995.
2. Tsinober A. *An Informal Conceptual Introduction to Turbulence*, 2nd ed.; Springer: Berlin/Heidelberg, Germany, 2009.
3. Zou WN. Recasting theory of elasticity with micro-finite elements. *Acta Mech. Sin.* **2015**, *31*, 679–684. DOI:10.1007/s10409-015-0488-4
4. Murdoch AI. *Physical Foundations of Continuum Mechanics*; Cambridge University Press: Cambridge, UK, 2012.

5. Kreuzer HJ. *Nonequilibrium Thermodynamics and Its Statistical Foundations*; Clarendon Press: Oxford, UK, 1981.
6. Tritton DJ. *Physical Fluid Dynamics*, 2nd ed.; Clarendon Press: Oxford, UK, 1988.
7. Chern S-S, Chern W-H, Lam KS. *Lectures on Differential Geometry*; World Scientific Pub.: Singapore, 2000.
8. Ackerson BJ, Pusey PN. Shear-Induced Order in Suspensions of Hard Spheres. *Phys. Rev. Lett.* **1988**, *61*, 1033–1036. DOI:10.1103/PhysRevLett.61.1033
9. Xue W, Grest GS. Shear-induced alignment of colloidal particles in the presence of a shear flow. *Phys. Rev. Lett.* **1990**, *64*, 419–422. DOI:10.1103/PhysRevLett.64.419
10. Edelen DGB. *Applied Exterior Calculus*; John Wiley Sons, Inc.: New York, NY, USA, 1985.
11. Batchelor GK. *An Introduction to Fluid Dynamics*; Cambridge University Press: Cambridge, UK, 1985.
12. He J, Wang J, Kong QC, Zhao PL, Cai XS, Zhang XH, et al. Slip viscosity and strain-rate viscosity in Taylor-Couette laminar flows: Experimental falsification and end-wall effects. *arXiv* **2026**, DOI:10.48550/arXiv.2601.09319; to be published in *AIP Advances*, 2026.
13. Newton I. *The Principia: Mathematical Principles of Natural Philosophy*; Book 2 Sect. 9 (A New Translation by Cohen IB, Whitman A, assisted by Budenz J, from Latin version, 1687); University of California Press: Berkeley, CA, USA, 1999.
14. Smith GE. Newton's study of fluid mechanics. *Int. J. Eng. Sci.* **1998**, *36*, 1377–1390. DOI:10.1016/S0020-7225(98)00038-X
15. Taylor GI. Distribution of velocity and temperature between concentric rotating cylinders. *Proc. R. Soc. London A* **1935**, *151*, 494–512. DOI:10.1098/rspa.1935.0163
16. Taylor GI. Fluid friction between rotating cylinders I—Torque measurements. *Proc. R. Soc. Lond. A* **1936**, *157*, 546–564. DOI:10.1098/rspa.1936.0215
17. Taylor GI. Fluid friction between rotating cylinders II—Distribution of velocity between concentric cylinders when outer one is rotating and inner one is rest. *Proc. R. Soc. Lond. A* **1936**, *157*, 565–578. DOI:10.1098/rspa.1936.0216
18. Schlichting H. *Boundary-Layer Theory*, 7th ed.; Kestin J, Translator; McGraw-Hill Book Co.: Columbus, OH, USA, 1979.
19. van Gils DPM, Bruggert GW, Lathrop DP, Sun C, Lohse D. The Twente turbulent Taylor–Couette (T3C) facility: Strongly turbulent (multiphase) flow between two independently rotating cylinders. *Rev. Sci. Instrum.* **2011**, *82*, 025105. DOI:10.1063/1.3548924
20. Huisman SG, van Gils DPM, Sun C. Applying laser Doppler anemometry inside a Taylor–Couette geometry using a ray-tracer to correct for curvature effects. *Eur. J. Mech. B/Fluids* **2012**, *36*, 115–119. DOI:10.1016/j.euromechflu.2012.03.013